ISSN 1392–1320 MATERIALS SCIENCE (MEDŽIAGOTYRA). Vol. 21, No. 3. 2015

Temperature Distribution Simulation of a Polymer Bearing Basing on the Real Tribological Tests

Artur KRÓL [1]*, Krzysztof KASZA [2]

[1] *Military University of Technology, Faculty of Mechanical Engineering, Gen. Kaliskiego St. 2, 00-908 Warsaw, Poland*
[2] *ABB Sp z o.o., Corporate Research, Starowiślna St. 13A, 31-038 Cracow, Poland*

crossref http://dx.doi.org/10.5755/j01.ms.21.3.7342

Received 16 June 2014; accepted 26 February 2015

The paper presents an attempt of temperature distribution simulation of a polymer bearing. In order to create model, tribological tests were performed and thermal behavior of the bearing was observed until temperature constant values were achieved. Thermal simulations were done with commercial software package ANSYS Fluent for 3D geometrical model that included polymer bearing, its housing, shaft and some volume of the surrounding air.
The heat generation caused by friction forces was implemented by volumetric heat source. The heat transfer and dissipation was through conduction, radiation and convection. The numerical model included all three mechanisms and in case of convection the heat transfer coefficient was not estimated by directly solved basing on the air flow around the bearing and adjacent parts.
Keywords: polymer bearing, thermal distribution, thermal simulations.

1. INTRODUCTION

Polymer bearings are widely used in tribological pairs due to dry-lubrication mechanism, low weight, corrosion resistance and maintenance-free operation [1, 2]. They are applied in different tribological pairs, i.e. household appliances, mechatronics systems, medical devices, food machines and many more. However, their use is limited by high coefficient of thermal expansion and softening at elevated temperature, especially when working outside recommended *pv* factors, where *p* is the pressure from bearing load, *v* is the sliding velocity of the shaft. Thus, a heat transfer in a real tribological pair with polymer bearing always needs special consideration as viscoelastic materials are very sensitive to frictional heating. Heat generation, converted from mechanical energy, could result in deformation, hysteresis, dispersion, viscous flow and creation or breakdown of adhesion bonds [3]. Finally, temperature during operation could strongly impact on the wear and friction of polymer bearings.

The modification of bearing design to achieve better characteristics at more demanding conditions requires full understanding of mechanical and thermal phenomena of bearing work. Computer simulations are very useful tool for complex product's analysis and they become more and more common among design engineers. Although, in the end they are often used for replacing of real experiments, it is much valuable, if some amount of experimental data are used for model development and validation of the obtained results.

Temperature distribution in a polymer bearing may be analyzed by application of analytical or mathematical models as well as numerical (finite element) methods. The example of analytical approach is presented in [4] and authors compare the obtained results with the experimental data and with the results from numerical model proposed in [5]. The authors of [6] also presents mathematical model of polymeric sliding bearing for analysis of effect of low climate temperature on heat dissipation distribution and finally the proposed calculation algorithm is numerically solved using finite difference method. On the other hand, the application of general purpose CFD code for complex 3D analysis of hydrodynamic journal bearing is discussed in [7]. It is demonstrated, that the CFD approach allows analysis more complex structures and more detailed description of physical phenomena.

Provided references are only a few examples of literature related to thermal modelling of bearings. However, it seems that numerical analysis of polymer, lubricant-free bearings is not common subject. The aim of the presented work is development and testing of the numerical model for thermal analysis of polymer sleeve bearing, basing on commercially available CFD code. Such model, after its positive validation, is intended to help in development of the new design concepts.

2. EXPERIMENTAL DETAILS

The test bearing in pillow block configuration is presented in Fig. 1. The bearing diameter and width at the contact surface with shaft was 1-7/16" and 1-5/16" respectively. The contact with housing was at diameter ~ 2.828" and with 13/16". Material of the tested bearing was Delrin 510MP by DuPont, acetal resin with 10 % of PTFE Micropowder [8] The first step was to observe a thermal behavior of polymer bearing under real test conditions on the stand tester (Fig. 2), equipped with three thermocouples (K-Type) and load sensor to measure moment of friction and also humidity and rotational speed sensor.

Firstly, the tests were performed under applied load of 300 N at increased rotational speed (100, 200 and 300 rpm) and at the end velocity was decreased to 100 rpm.

* Corresponding author. Tel.: +48-22-6839410; fax: +48-22-6837366.
E-mail address: *artur.krol@wat.edu.pl* (A. Król)

Secondly the tests under load of 750 N were carried out at smaller rotations, i.e. 50, 100, 150 and again 50 rpm. Each study was continued until constant values were achieved, i.e. temperature and moment of friction. Load parameters (force and angular velocity) used in experiments were arbitrary selected by authors basing on data about bearing lifetime. The goal was to minimize influence of bearing wear on temperature results.

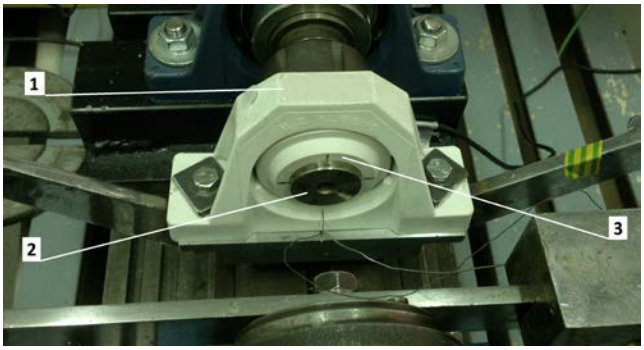

Fig. 1. The test cell: 1 – housing, 2 – shaft, 3 – polymer bearing

Fig. 2. View of the tribological tester with measuring equipment (1 – DC electric motor, 2 – supporting bearings with the holder of tested shaft, 3 – humidity sensor and rotational speed sensor, 4 – load system: two symmetric weight levers and measuring arm of friction moment, 5 – computer and measuring systems of electric signals from three thermocouples and load sensor, 6 – test cell: tribological pair of stainless shaft and polymer bearing)

Significant matter to consider was a mounting of K-type thermocouples. Two of them were located in the bearing body (Fig. 3): *T1* – 1.8 mm from the bearing-shaft friction area and *T2* – 3.2 mm from the friction area, through channels drilled in the housing and in the bearing.

The third thermocouple *T3* was mounted in the housing at the crossroad of housing and bearing insert.

Before each test polymer sliding bearing was prepared for the thermocouple mounting. Appropriate channels were drilled in each polymer sleeve and housing and their size and location are explained in the Fig. 3 and Fig. 4.

A few thermographic pictures were also taken during the test with load value 750 N, using thermal camera MobIR M8. These IR photos provided general view on temperature distribution in the bearing and its housing and the example is shown in Fig. 12. However, due to unknown exact value of emissivity of materials thermographic pictures were mainly used for qualitative comparison of experimental measurements and numerical results.

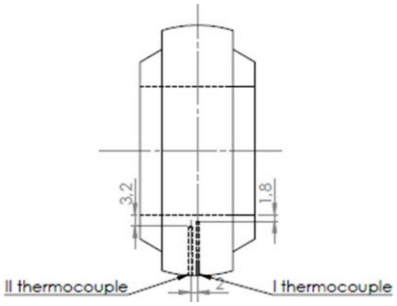

Fig. 3. Schematic view of thermocouple location in the polymer bearing (*T1* and *T2*)

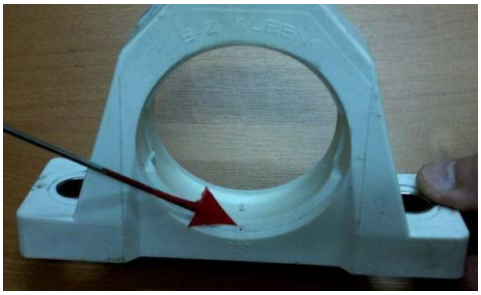

Fig. 4. The photo with indicated location of thermocouple (*T3*) in the housing of the bearing

3. RESULTS OF EXPERIMENTS

In Fig. 5 example results of the tests are presented under load of 300 N with three curves from the used thermocouples (*T1*, *T2* and *T3*) and with curve of friction coefficient μ calculated according to the formula:

$$\mu = \frac{2 \cdot M_f}{P \cdot d}, \tag{1}$$

where: M_f is the moment of friction, N·m; P is the axial load acting on the bearing, N; d is the inside diameter of the bearing, m.

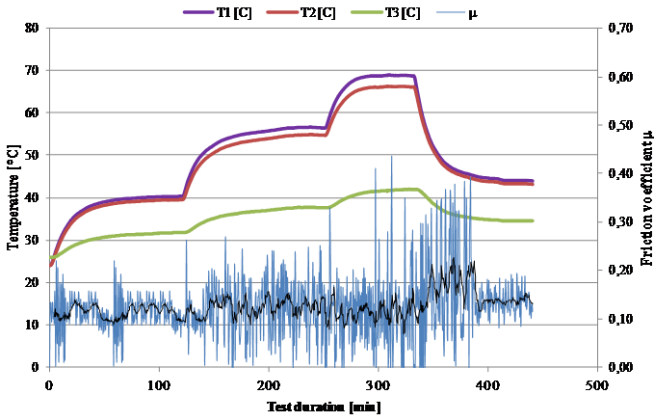

Fig. 5. Example results of polymer bearing test under load of 300 N and at rotational speed 100, 200, 300 and 100 rpm: *T1*, *T2*, *T3* – curves of temperature, μ – curve of friction coefficient with the averaged curve

Consequently, in Fig. 6 results of the test under load of 750 N are presented at the rotational speed 50, 100, 150 and 50 rpm.

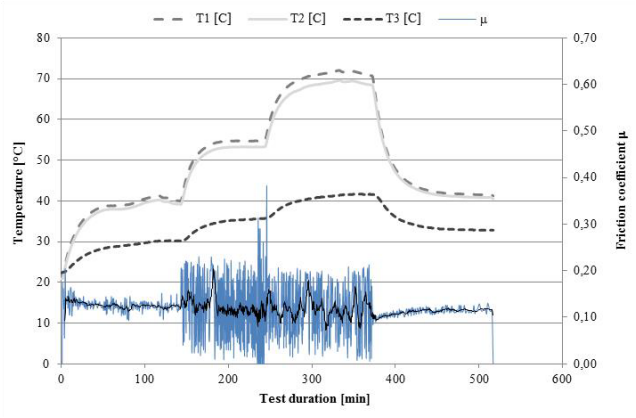

Fig. 6. Example results of polymer bearing test under load of 750 N and at rotational speed 50, 100, 150 and 50 rpm: *T1*, *T2*, *T3* – curves of temperature, μ – curve of friction coefficient with the averaged curve

In Fig. 7 and Fig. 8 summarized results of stable parameters of the bearing work are presented.

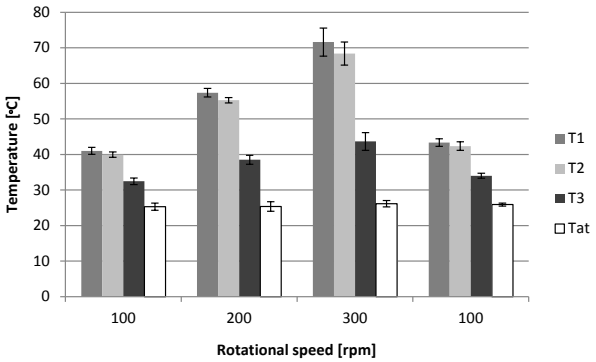

Fig. 7. Summarized results of temperature measurement for the test under load of 300N and at rotational speed 100, 200, 300 and 100 rpm: *T1*, *T2*, *T3* – temperature from thermocouples, *T*at – ambient temperature

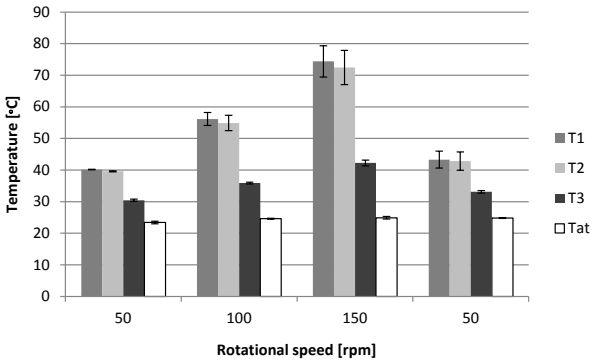

Fig. 8. Summarized results of temperature measurement for the test under load of 750 N and at rotational speed 50, 100, 150 and 50 rpm: *T1*, *T2*, *T3* – temperature from thermocouples, *T*at – ambient temperature

It is clearly seen that increase of rotational speed resulted in rather proportional raise of the polymer bearing temperature. Analysis of that data shows also that increase of temperature under load of 750 N was higher than under load of 300 N.

Discussing results of friction coefficient measurement and calculation (Fig. 9) it could be noticed that average value of the parameter was dependent on the load and rotational speed. However it is noticeable that value of friction coefficient under 750 N was considerably higher.

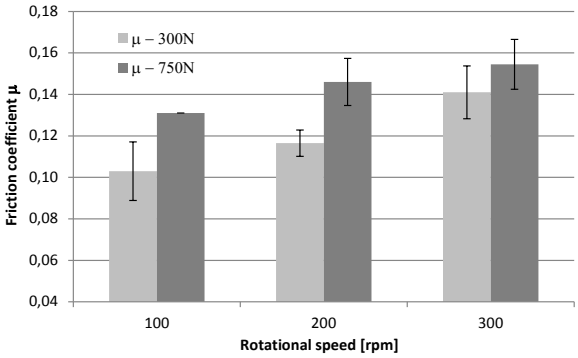

Fig. 9. Summarized results of friction coefficient μ measurement and calculation for the tests under load of 300 N and 750 N

4. NUMERICAL MODEL AND ITS VALIDATION

The achieved results of the measurements were used for development and validation of numerical model for temperature distribution in polymer bearing. Computer simulation are useful engineering tool that in case of polymer bearing may provide more detailed information about thermal distribution and heat transfer during its operation. The essential advantage of numerical model is ability to analyse temperature distribution in the whole object volume and not only in selected and limited number of measurement points. The other benefit is an easy preliminary testing of new desing concepts without necessity of prototype manufacturing.

The shaft, sleeve polymer bearing with its housing and limited volume of the surrounding air are the elements of the experimental stand that were included in the Computational Fluid Dynamics (CFD) analysis. The 3D geometrical models of these parts are shown in Fig. 10.

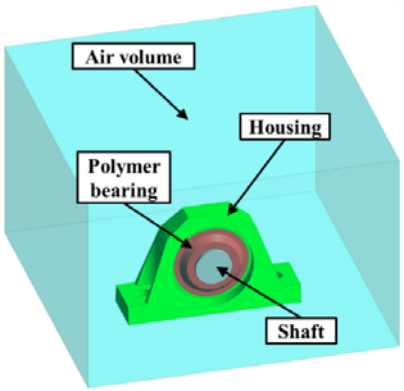

Fig. 10. Representation of the experimental stand in 3D CAD geometry

The preparations of the numerical mesh, setup of CFD model as well as all calculations were done using the commercial software package ANSYS Fluent [9 – 11]. The software provides mathematical models and solver for analysis of mass and heat transfer phenomena. The finite volume mesh consisted of about 1.2 millions of elements.

Thermal analysis of the polymer bearing problem could be solved using only energy conservation equation:

$$\frac{\partial}{\partial t}(\rho h) = \nabla \cdot (k \nabla T) + S_h, \quad (2)$$

where ρ is the density, h is the enthalpy, k is the thermal conductivity, T is the absolute temperature, t is the time and S_h is the energy source. However, that would require definition of boundary conditions directly on the surface of the solid elements by specifying temperature, heat flux or surface heat transfer coefficient together with temperature of the surrounding air. Different approach is proposed in the presented case. These boundary conditions do not have to be defined because the model geometry includes a representative volume of the surrounding air and its flow around all solid parts with as well as local heat transfer coefficients are directly solved. The additional required mass (3), momentum (4) and energy (5) conservation equation for fluid volume are:

$$\frac{\partial \rho}{\partial t} + \nabla \cdot (\rho \vec{v}) = S_m; \quad (3)$$

$$\frac{\partial}{\partial t}(\rho \vec{v}) + \nabla \cdot (\rho \vec{v} \vec{v}) = -\nabla p + \nabla \cdot (\tau) + \rho \vec{g} + \vec{F}; \quad (4)$$

$$\frac{\partial}{\partial t}(\rho E) + \nabla \cdot (\vec{v}(\rho E + p)) = \nabla \cdot \left(k \nabla T - h \vec{J} + (\tau \cdot \vec{v})\right) + S_h, \quad (5)$$

where v is velocity, S_m is mass source, p is pressure, τ is stress tensor, g is gravitational acceleration, F is related to external forces, E is total energy and J is mass or diffusion flux. It has to be pointed out that in the considered case the air flow is in major part caused by natural convection and thus gas density must be specified as temperature dependent [12]. The other air properties like dynamic viscosity, heat capacity and thermal conductivity were also defined as a function of temperature [12]. The material properties of solid elements (i.e. density, heat capacity and thermal conductivity) were constant due to lack of appropriate data and they are listed in Table 1.

Table 1. Thermal properties of solid parts

Part	Density, kg/m^3	Heat Capacity, J/kgK	Thermal Conductivity, W/mK
Shaft	8030	502.48	16.27
Bearing	1480	1000	0.32
Housing	1530	1000	0.28

The additional phenomena like turbulent air flow and radiation were also part of the CFD model. The relevant equations are not presented in this paper but they may be found in literature together with detailed explanation [10, 11]. ANSYS Fluent offers a large number of choices and in the considered case Discrete Ordinates (DO) Radiation Model [13, 14] was used together with Spalart-Allmaras model [15] for turbulence calculation. The radiation model required specifying of emissivity. It was already mentioned that exact values were not known. In the proposed model they were assumed basing on available literature data and authors' experience: 0.95 at external walls of representative air volume and at polymer surfaces, 0.2 at front surface of the shaft and 0.1 at its side surface.

The main boundary conditions in the proposed model were pressure and temperature value at the walls of air geometry, which were responsible for heat dissipation and heat source at contact surface between the shaft and polymer bearing. The pressure and temperature value were set according to ambient conditions recorded during the experiments – 1000 hPa and 20 °C. The heat source was defined by a function, which specified its distribution along the circumference of the contact surface. The shape and area of the actual contact surface in the experiments was not known. The proposed function allowed testing of different heating options.

The example simulations results are shown in Fig. 11. The picture presents temperature distribution at the surface of the shaft, polymer bearing and its housing as well as streamlines of air natural convection flow. The maximum temperature is at the contact surface between shaft and bearing. The shaft has very uniform temperature distribution due to high thermal conductivity of steel. In contrary, large temperature gradients may be observed in polymer bearing and its housing, which are the effect of low thermal conductivity of these materials.

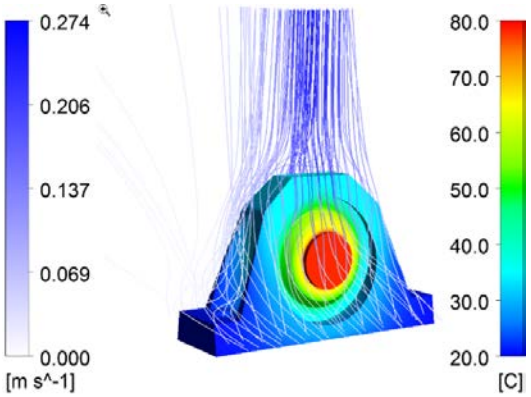

Fig. 11. Example simulation results: temperature distribution at shaft, bearing and housing with streamlines of air flow

In Fig. 12 the results from computer simulations and infrared measurements are compared for one selected load and velocity value. Temperature distribution and temperature values are similar. It must be explained that low temperature at the shaft surface observed on infrared picture is caused by lower emissivity of that area. For that reason shaft temperature is not shown on bottom image.

The example comparison of selected measurement points for the same load conditions (750 N and 150 rpm) are presented in Table 2. The values represent measured and calculated temperature rise above ambient conditions. The relative error is percentage difference between these results in reference to the measured temperatures**.** The obtained agreement between the measured and calculated values is very good for points *T1*, *T2* and *T3*. In other locations differences were higher, but still they are reflecting thermal behavior of the bearing. It is assumed that these inaccuracies may be caused by both measurement uncertainties as well as geometry simplifications and parameters of the numerical model.

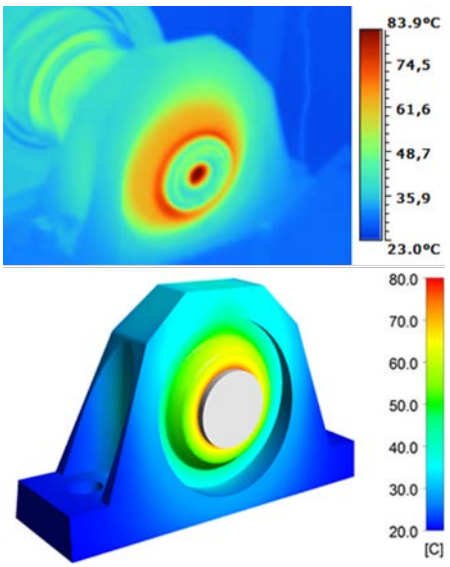

Fig. 12. Temperature distribution from infrared camera (top) and computer simulations (bottom). Load value 750 N and angular velocity 150 rpm

The points *T1-T3* were measured using thermocouple sensors while for all others, temperature value was estimated basing on infrared pictures. Measurement points *T1-T3* are also very close to heating source in the simulation model and far from boundary conditions. That makes them less sensitive to these model parameters as well as material properties of the solid parts.

Table 2. Comparison of measured and computed temperature rise (ΔT) at selected positions

Measurement point	Measured ΔT in K	Calculated ΔT in K	Relative error in %
T1	52.9	52.8	0.19%
T2	51.4	49.6	3.50%
T3	18.0	18.2	1.11%
Housing top – E	23.7	16.8	29.11%
Housing top side – F	19.7	10.7	45.69%
Housing top side – F'	20.7	10.8	47.83%
Shaft	68.3	58.4	14.49%

5. CONCLUSIONS

Experiments with polymer bearing exposed to different load and velocity conditions were performed in order to record temperature distribution at selected locations. Measurement results were used for validation of the proposed three dimensional numerical model of the polymer, lubricant-free sleeve bearing, which was based on the commercial CFD code ANSYS Fluent. The calculated and measured temperature distribution were similar. However, much higher accuracy (the error lower than 4 %) was achieved in the area of heat generation – close to contact surface between the bearing and shaft. In other location, e.g. on the housing of the bearing, discrepancies between simulation and experimental results were between 15 – 50 %. The source of higher error was not identified and could be related to both calculation and measurement accuracy. The calculation accuracy could be influenced by for example simplifications in model geometry or description of material properties. In case of temperature measurements it would be recommended to use more local temperature sensors (e.g. thermocouples) instead of IR camera. Nevertheless, it is judged that the proposed model may be used for qualitative analysis of thermal behavior of the polymer plain bearing and preliminary evaluation of new design concepts. It is also assumed that the calculation accuracy may be further improved, but it would require additional steps in development of the numerical model like for example so called sensitivity analysis for model parameters such as material properties or boundary conditions.

REFERENCES

1. **Lawrowski, Z.** Polymers in the Construction of Serviceless sliding bearings *Archives of Civil and Mechanical Engineering* 7 (4) 2007: pp. 139 – 150. http://dx.doi.org/10.1016/S1644-9665(12)60232-5
2. **Ünlü, B. S., Atik, E., Köksal, S.** Tribological Properties of Polymer-based Journal Bearings *Materials & Design* 30 (7) 2010: pp. 2618 – 2622.
3. **Myshkin, N. K., Petrokovets, M. I., Kovalev, A. V.** Tribology of Polymers: Adhesion, Friction, Wear, and Mass-transfer *Tribology International* 38 2005: pp. 910 – 921. http://dx.doi.org/10.1016/j.triboint.2005.07.016
4. **Komanduri, R., Zhen Bing, H.** Thermal Analysis of Dry Sleeve Bearings – a Comparison Between Analytical, Numerical (Finite Element) and Experimental Results *Tribology International* 34 2001: pp. 145 – 160.
5. **Kennedy, F. E. Jr.** Surface Temperature in Sliding Systems – a Finite Element Analysis *Trans ASME, Journal of Tribology* 103 1981: pp. 90 – 96. http://dx.doi.org/10.1115/1.3251620
6. **Starostin, N. P., Kondakov, A. S., Dedyukin, A. E.** Effect of Low Climate Temperature on Heat Dissipation Distribution in Polymeric Sliding Bearing *Journal of Friction and Wear* 33 2012: pp. 415 – 421.
7. **Uhkoetter, S., Wiesche, S., Kursch, M., Beck, C.** Development and Validation of a Three-Dimensional Multiphase Flow Computational Fluid Dynamics Analysis for Journal Bearings in Steam and Heavy Duty Gas Turbines *Journal of Engineering for Gas Turbines and Power* (134) 2012: pp. 102504-8; doi:10.1115/1.4007078.
8. **DuPont Product Information –** http://plastics.dupont.com/plastics/pdflit/americas/delrin/H81093.pdf
9. www.ansys.com
10. FLUENT Theory Guide, Release 15.0, 2014, SAS IP, Inc.
11. FLUENT User's Guide, Release 15.0, 2014, SAS IP, Inc.
12. *VDI-Wärmeatlas: Berechnungsblätter für den Wärmeübergang* Springer (1997)
13. **Chui, E. H., Raithby, G. D.** Computation of Radiant Heat Transfer on a Non-Orthogonal Mesh Using the Finite-Volume Method *Numerical Heat Transfer* 23 1993: pp. 269 – 288. http://dx.doi.org/10.1080/10407799308914901
14. **Raithby, G. D., Chui, E. H.** A Finite-Volume Method for Predicting a Radiant Heat Transfer in Enclosures with Participating Media *Journal of Heat Transfer* 112 1990: pp. 415 – 423.
15. **Spalart, P., Allmaras, S.** A One-equation Turbulence Model for Aerodynamic Flows *Technical Report AIAA-92-0439, American Institute of Aeronautics and Astronautics* 1992.